ELSEVIER
Marine Micropaleontology 37 (1999) 1–22
MARINE MICROPALEONTOLOGY
www.elsevier.com/locate/marmicro

Pleistocene fluctuations in the Agulhas Current Retroflection based on the calcareous plankton record

José-Abel Flores [a,*], Rainer Gersonde [b], F. Javier Sierro [a]

[a] *Departamento de Geología, Universidad de Salamanca, Salamanca, Spain*
[b] *Alfred Wegener Institute for Polar and Marine Research, Bremerhaven, Germany*

Received 18 November 1998; accepted 24 February 1999

Abstract

Piston core (PS2487-6), recovered south of Cape Town, and sediment surface samples, recovered in the area of the Agulhas Current retroflection, were used to construct paleoceanographic scenarios for the late Quaternary in a region with an important role in global water mass transfer. Coccolithophore (calcareous nannofossil) and planktonic foraminifera assemblages and oxygen isotope data were collected. Stratigraphic control is based on calibration of the $\delta^{18}O$ stratigraphic signals with calcareous nannofossil events that are thought to be synchronous over a broad range of latitudes. Study of the surface sediments permits the characterisation of the Agulhas Current, Subtropical Convergence and Subantarctic coccolithophore assemblages. The Agulhas Current assemblage has relatively high proportions of *Florisphaera profunda*, *Gephyrocapsa oceanica* and *Umbilicosphaera* spp. These species are absent or present in low proportions in subantarctic waters. The abundance of coccolithophores during isotope stages 1, 5 and 7 is characteristic of relatively warm, stratified surface waters, with a deep nutricline and chlorophyll maximum, which strongly suggests that the area was under the influence of the Agulhas Current retroflection. The incursion of *Globigerinoides ruber*, abundant today in the Agulhas Current, also supports this interpretation. Conversely, during glacial stages 2–4 and 6, a strong reduction in warm and stratified water indicators can be observed, together with an increase in cold-eutrophic species.

The interval from isotope stages 8 to 12 displays an assemblage dominated by *Gephyrocapsa caribbeanica*, the highest values being seen in the so-called Mid-Brunhes event, accompanied by a clear reduction in subtropical Holocene species. During the glacial interval from isotope stages 10–12, *G. caribbeanica* dominated the assemblage. The ecological interpretation of this species is controversial due to a clear evolutionary overprint. Isotope stage 12 is here interpreted as having been the coldest one in the period studied. It is characterised by a strong increase in *Neogloboquadrina pachyderma* (dextral and sinistral) and a remarkable decrease in tropical and subtropical planktonic foraminifera. From isotope stage 13 to 18, a hiatus is interpreted. Below this hiatus the stratigraphic resolution is poorer, although the glacial–interglacial cyclicity is well defined in the Agulhas Current Retroflection area (Core PS2487-6) for the last 25 isotope stages. The glacial–interglacial cyclicity is thought to be due to a fluctuation in the Subtropical Convergence Zone, probably linked to the eastward and westward displacement of the Agulhas Current retroflection. In any case, the core studied was always in a subtropical environment, under the influence of the Agulhas Current, which was enhanced during interglacial periods. For the whole of the interval studied, increases in *Calcidiscus leptoporus*, *Umbilicosphaera* spp., and *Syracosphaera* spp. among the calcareous nannofossils, and in *G. ruber* and *Globigerinoides sacculifer* within the planktonic foraminifera,

---

[*] Corresponding author. E-mail: flores@gugu.usal.es

PII: S0377-8398(99)00012-2

clearly respond to interglacial pulses, reaching maximum values during short periods close to the major deglaciations.

Keywords: calcareous nannofossils; planktonic foraminifera; Pleistocene; South Atlantic; Agulhas Current; paleoceanography; oxygen isotope stratigraphy; biostratigraphy

1. Introduction

1.1. Oceanographic setting

The Agulhas Basin is located in the interconnecting region between the Indian and Atlantic oceans. The main oceanographic feature of the region is the Agulhas Current (AC), a warm water mass which marks the western boundary of the South Indian Ocean subtropical gyre. The AC flows southwestwards parallel to the East African coast. After entering the Atlantic Ocean, it returns eastward into the Indian Ocean (Agulhas Return Current) (Fig. 1; Lutjeharms, 1981, 1996). The tropical AC is characterised by temperatures higher than 17ºC and salinities lower than 35.5‰; the Subtropical Water can be distinguished by lower temperatures (less than 17ºC) and slightly higher salinities (more than 35.5‰) (Hutson, 1980). These features are easy to identify with satellite imagery (Lutjeharms and Valentine, 1984). The AC may reach depths down to 2500 m (Winter and Martin, 1990) and consists of an upper ‘thermohaline’ and a deeper intermediate water mass (the coldest Antarctic Intermediate Water) (Gordon et al., 1992). The southernmost boundary of the AC is sometimes defined by the Subtropical Convergence Zone (STCZ) (Lutjeharms and Valentine, 1984). According to Sverdrup et al. (1942), in this region the denser Subantarctic Surface Water subducts northwards beneath the Subtropical Water to form the South Atlantic and the Indian Central Water. This region defines a boundary which separates warm saline subtropical water from cool, low-salinity subpolar waters (Prell et al., 1979). South of Africa, today’s estimated mean temperature is 14.2ºC (Lutjeharms and Valentine, 1984); in this area the STCZ is placed at 42ºS, with a drop in temperature of 8.4ºC (Lutjeharms, 1981). Anticyclonic warm water eddies of the AC, generated in the retroflection regime, penetrate south of the Atlantic Ocean and represent a mechanism for interbasin heat exchange (Lutjeharms, 1981, 1996; Lutjeharms et al., 1981; Lutjeharms and Meeuwis, 1986; Schumann, 1987; Shannon et al., 1990; Gordon et al., 1992; Shannon and Nelson, 1996; Fu, 1996). In the Atlantic Ocean, west of Africa, the STCZ is located south of 40ºS. In this area southwest of Africa, the Benguela Current (BC), as a branch of the South Atlantic Current limited southeast by the Agulhas Front (defined between 13 and 25ºE), is the most significant feature (Strama and Peterson, 1990; Strama, 1991; Lutjeharms et al., 1992) and is responsible for coastal upwelling (Lutjeharms, 1981). In general, the BC can be distinguished from neighbouring subtropical water masses by low surface water temperature and salinity (Giraudeau, 1992).

The surface water characteristics in the AC region have been described by Gordon et al. (1987), who reported the presence of different waters from the Indian Ocean. The Indian Ocean Tropical Surface Water is characterised by temperatures warmer than 22ºC and salinities below 35.0‰. The Subtropical Surface and Tropical Thermocline waters are characterised by higher salinities. Other important features of these tropical waters are a strong degree of stratification, with an oxygen minimum and high nutrient content at 200 m (deep nutricline), and well-stratified surface waters (Warren, 1981). These characteristics are also identified in eddies generated in the AC retroflection (Gordon et al., 1987), although a progressive degree of alteration occurring during their northward displacement (Chapman et al., 1987). The AC surface waters and related eddies show a clear stratification, the nutricline and Depth Chlorophyll Maximum being situated at about 100 m depth (Chapman et al., 1987).

1.2. Objectives

As an interbasin area connecting two oceans, the Agulhas Basin is a critical region in the global pattern of heat transport (Gordon, 1986; Broecker,

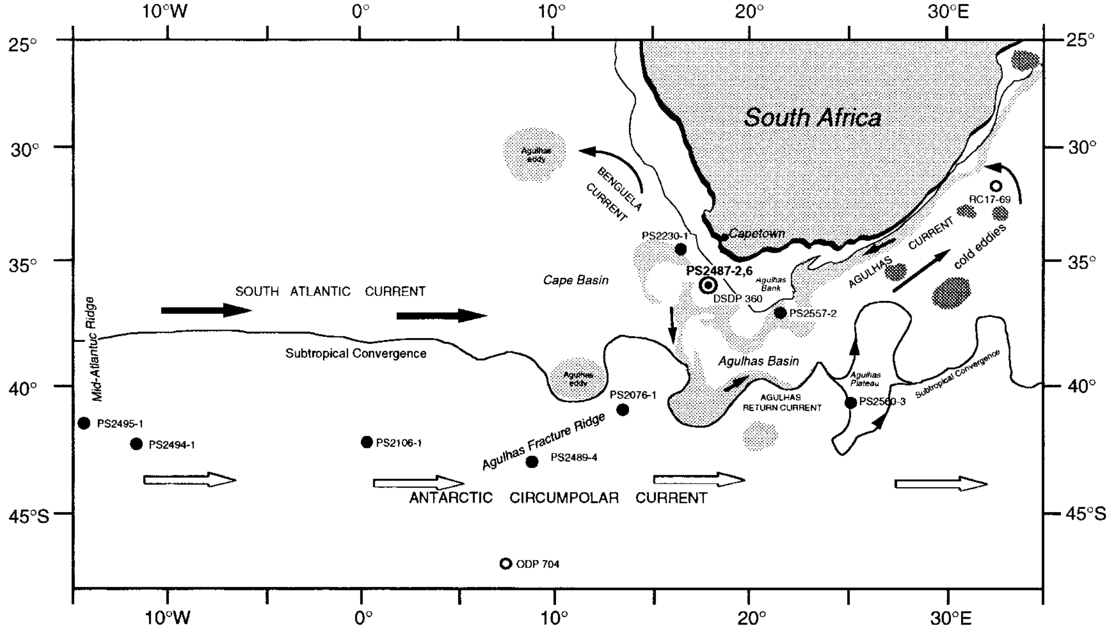

Fig. 1. Map of the Agulhas Current retroflection area and main conceptual oceanographic features (after Lutjeharms, 1981). The large dot represents the core studied and the small dots show the position of the surface sediment samples used in this study. Significant sites referred to in the text (Core RC17-69, DSDP Site 360 and ODP Site 704) are represented as circles.

1987, 1991; Gordon et al., 1992; Wefer et al., 1996). Changes in the southern boundary of the AC could have increased or decreased its activity and hence may have modified the heat budget and the paleoceanography of the region (Fig. 1). Micropaleontological and biochemical information about the region is scanty due to limitations in the number and quality of cores available and, in general, these show significant hiatuses and low sedimentation rates. The core studied here provides a relatively continuous succession in the AC retroflection area.

This study had the following goals: (1) to establish a medium-resolution nannofossil stratigraphy for the Pleistocene sediments recovered in order to interpret the $\delta^{18}O$ signal; (2) to analyse the evolution of the nannofossil assemblages and correlate their characteristics with those of other paleoenvironmental proxies, in order to reconstruct the surface water mass characteristics; and (3) to reconstruct the history and dynamics of the AC retroflection area during the Late Pleistocene.

2. Previous work

Martin et al. (1982) argued that the AC has been a general feature of the Indian Ocean circulation since the middle Tertiary. Hutson (1980), studying foraminifera in Core RC 17-69, suggested that during glacial events the AC was replaced by cooler subtropical water masses in winter months, with a weak development during summer months. Prell et al. (1980), using the same core, reported that at the Last Glacial Maximum the AC was cooler, probably shallower, and subject to considerable seasonal variation. In this case, heat transfer from the tropical to temperate latitudes may have been reduced (Winter and Martin, 1990).

The position of the STCZ has fluctuated during the Late Pleistocene. Bé and Duplessy (1976) suggested a maximum displacement of 10° northward for the last 540,000 yr, whereas Prell et al. (1979, 1980) estimated that during glacial periods the STCZ moved northward only 2°. Both Bé and Duplessy (1976) and Prell et al. (1979) studied Core RC 17-69, which, according to Winter and Martin

(1990), is not well positioned to study the evolution of the AC. Martin and Flemming (1988) concluded that it is not feasible to propose that the AC would have deviated strongly from the present flow during low-sea levels (glacial periods) because of the proximity of the African slope. Also, it is important to consider the area where Core RC 17-69 was recovered, where different water masses are mixed in eddies (Gründlingh, 1985, 1986).

Winter and Martin (1990) studied the $\delta^{18}O$ isotope record and coccolithophore assemblages in several cores situated in the present day AC area. They concluded that during the last 150,000 yr the shifts observed in the coccolithophore assemblage may reflect changes in upwelling plumes and eddy formation, related to winter cooling.

In the BC area, Giraudeau (1992, 1993) studied the coccolithophore and planktonic foraminifera assemblages from sediment surface samples and reported the correspondence between several species and hydrographical parameters in this upwelling regime.

In the Subantarctic region (ODP Site 704), Gard and Crux (1991) studied the coccolithophore assemblage and its fluctuation during glacial–interglacial periods. Hodell (1993), in the same ODP site, and Howard and Prell (1992), in the Southern Indian Ocean, interpreted fluctuations of the Polar Front Zone (PFZ) and STCZ during the Late Pleistocene.

3. Material and methods

Piston Core PS2487-6 (35º49.2′S, 18º05.4′E; 2950 m depth) was recovered during the RV *Polarstern* expedition ANTARKTIS-XI/2 during the 1993/1994 austral summer (Gersonde et al., 1995). The core, which was recovered at the location of DSDP Site 360 (Bolli et al., 1978), has a total length of 12 m. The lithology is a foraminifera ooze alternating with mud and nannofossil ooze (Fig. 2). A sampling interval of 5–10 cm was used for the micropaleontological and geochemical studies.

As well as downcore studies, additional surface sediment samples (Holocene) were recovered using Multicorer and Minicorer systems (AWI-Minicorer; Gersonde et al., 1995) to collect data on the modern distribution of representative coccolithophore assemblages (Table 1). Two different domains were studied: Subtropical (linked to the AC) and Subantarctic. Samples from the STCZ area were also studied. These samples were recovered in two NW–SW and E–W transects during RV *Polarstern* expeditions ANTARKTIS-IX/4 (1991), X/4 (1991/1992), XI-2 (1993/1994), and XI/4 (1994) (Fig. 1; Table 1).

Nannofossil slides for core and surficial sediment samples were prepared using the technique of Flores and Sierro (1997), which allows collection of uniform and comparable data between different samples, and the estimation of total nannofossil abundances (nannofossils per g). Coccolithophore analyses were made at ×1250 magnification using a polarised light microscope. For slide preparation, the weight of sediment, the surface over which the sediment was uniformly distributed and the observed surface was controlled, allowing conversion of the number of nannofossils per surface area (nannofossils per mm^2) into nannofossils per gram of sediment.

These slides are stored in the archives of the Micropaleontological Collections of the University of Salamanca and the Alfred Wegener Institute. For quantitative analysis, about 300 nannoliths larger than 3 μm were counted per slide in a varying number fields of view. Nannofossils smaller than 3 μm were counted separately in same number of fields of view. Species recorded at low proportions in the previous counting were counted in additional fields of view.

For biostratigraphic analysis, the relative abundances (percentages of the most abundant taxa) of selected species were used in order to avoid dilution effects and to compare our data with those previously published.

Additionally, routine Scanning Electron Microscope (SEM) analyses were performed in order to estimate the preservation state or morphological features of calcareous nannofossils.

For planktonic foraminifera analyses, 1 g of dried sediment was disintegrated in demineralised water and then washed through 125, 62 and 37 μm sieves. After drying, the 125 μm residue was weighed and split into different fractions using a microsplitter. Around 300 specimens were counted to estimate relative abundances. The absolute concentration of planktonic foraminifera was calculated by weighing the residue larger than 37 μm, consisting mainly

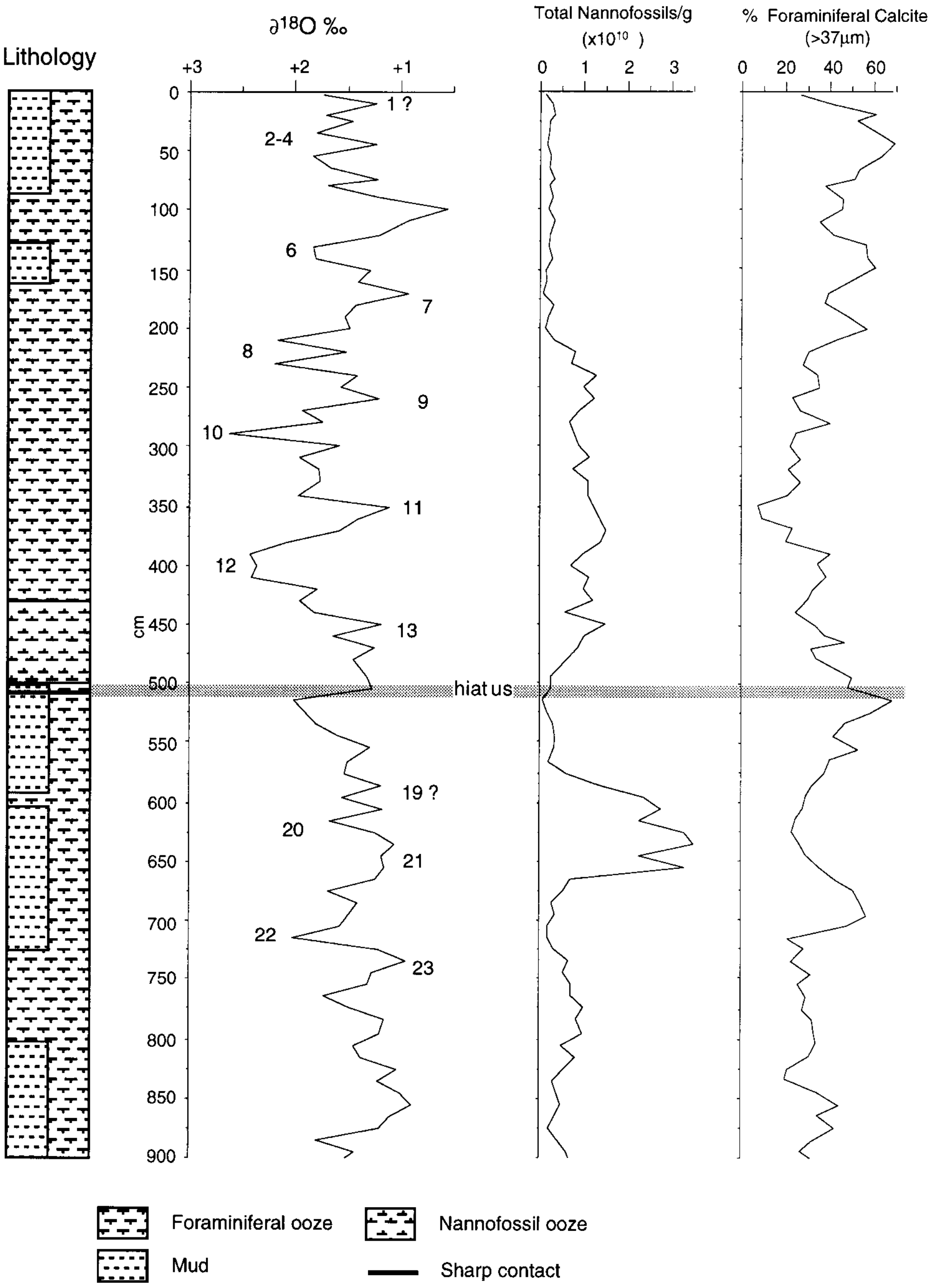

Fig. 2. $\delta^{18}O$ isotope curve, lithology, total nannofossils per gram and the percentage of foraminifera calcite (shells >37 μm) in Core PS2487-6. For counting details and procedure see text. Table 2 contains the numerical isotopic data.

of planktonic foraminifera, and estimating the percentage of this fraction in relation to the initial dry sample weight.

Five specimens of *Globorotalia inflata* ranging in size between 250 and 300 μm were picked from each residue for isotope analyses. The isotopic mea-

Table 1
Surface sediment sample location, depth and type

Core	*Polarstern* expedition	Sampling technique	interval (cm)	situation	depth (m)
PS2487-2	ANTARKTIS-XI/2 1993/1994	MUC	0–0.5	35º49′S, 18º05′E	2950
PS2557-2	ANTARKTIS-XI/4 1994	MUC	0–0.5	36º57′S, 21º47.04′E	3371
PS2230-1	ANTARKTIS-X/4 1991/1992	MIC	0–1	34º45′S, 17º22′E	2578
PS2560-3	ANTARKTIS-XI/4 1994	MUC	0–0.5	40º34′S, 25º35′E	3641
PS2076-1	ANTARKTIS-IX4 1991	MUC	0.5–1.5	41º08′S, 13º28′E	2086
PS2489-4	ANTARKTIS-XI/2 1993/1994	MUC	0–0.5	42º52′S, 08º58′E	3794
PS2106-1	ANTARKTIS-IX4 1991	MUC	0–0.5	41º51′S, 0º05′E	912
PS2494-1	ANTARKTIS-XI/2 1993/1994	MUC	0–0.5	41º41′S, 12º20′W	3324
PS2495-1	ANTARKTIS-XI/2 1993/1994	MIN	0–0.5	41º17′S, 14º30′W	3135

MUC = Multicorer; MIN = AWI-Minicorer.

surements were performed with a Finnigan Modern Analogue Technique (MAT) 251 mass spectrometer coupled to an automatic carbonate preparation device. Standard deviations of measurements were <0.09‰ for oxygen. Data were related to the PDB standard through repeated analyses of National Bureau of Standards isotopic reference material 19 (Hut, 1987).

4. Microfossil preservation

Calcareous nannofossil preservation within Core PS2487-6 can be considered good for the entire core; only minor dissolution features are observed in certain specimens. The rims of some placoliths, such as *Gephyrocapsa muellerae* and *Emiliania* morphotypes or the central area of *Syracosphaera* spp. and *Pontosphaera* spp. are weakly dissolved at some levels. These differences in preservation do not hamper the identification of taxa. It is also of note that in all the samples studied, easily dissolved specimens (e.g. very small placoliths and caneoliths) are present, although, and only occasionally, small specimens of *Emiliania huxleyi* and small *Gephyrocapsa* with lost bridges are difficult to distinguish by light microscope observation. In these cases, additional SEM analysis was carried out. Overgrowth is less significant than etching and is only observed in the central area of occasional specimens of *Coccolithus pelagicus,* large *Gephyrocapsa* and *Reticulofenestra asanoi*. No differences in preservation between interglacial and glacial episodes are observed. Reworked nannofossils from Miocene and Pliocene sediments are scarce.

Planktonic foraminifera preservation is excellent in the uppermost 2 m of the core, and good-to-moderate downcore, where the percentage of fragmentation clearly increases. However, the different species of planktonic foraminifera can always be easily identified even when the degree of fragmentation is high.

5. Results

5.1. δ^{18}O isotope curve interpretation and Pleistocene calcareous nannofossil stratigraphy

The δ^{18}O curve obtained with the *Globorotalia inflata* planktonic foraminifera was compared with

Table 2
δ^{18}O data set. Isotope analyses were obtained from *G. inflata* specimens

cm	δ^{18}O	cm	δ^{18}O
3	2.236	450	1.688
10	1.735	460	2.142
20	2.214	465	1.935
25	1.961	470	1.750
35	2.303	480	1.948
45	1.736	495	1.819
55	2.338	505	1.767
65	2.167	515	2.513
75	1.718	535	2.300
80	2.188	545	2.095
90	1.716	555	1.791
100	1.059	565	2.002
110	1.438	575	2.029
120	1.704	585	1.686
130	2.328	595	2.052
140	2.308	605	1.673
150	1.789	615	2.173
160	1.906	625	1.744
170	1.430	635	1.555
180	1.927	645	1.678
190	2.034	655	1.654
200	1.981	665	1.742
210	2.669	675	2.181
220	2.017	685	1.909
230	2.697	695	1.988
240	1.911	705	2.072
250	2.067	715	2.522
260	1.706	725	1.716
270	2.433	735	1.444
280	2.238	745	1.767
290	3.124	755	1.809
300	2.082	765	2.229
310	2.460	775	1.986
320	2.272	785	1.654
330	2.260	795	1.702
340	2.465	805	1.939
350	1.611	815	1.870
360	1.909	825	1.533
370	2.079	835	1.712
380	2.578	845	1.500
390	2.927	855	1.391
400	2.861	865	1.598
410	2.914	875	1.700
420	2.288	885	2.297
430	2.451	895	1.937
440	2.319	905	2.101

the calcareous nannofossil and foraminifera data in order to identify the isotope stages (Table 2). Fig. 2 shows the marine isotope stage (MIS) identified in Core PS2487-6. For the Late Pleistocene (after MIS 13), we used the isotope time scale of Martinson et al. (1987). For the lower part (before MIS 18) of the core, the isotopic stratigraphy is less accurate. In this lower interval we compared our calcareous nannofossil bioevents with those calibrated by Raffi et al. (1993) and Wei (1993), following the timescale of Shackleton et al. (1990).

The nannofossil events identified and the assigned ages are shown in Fig. 3. Taxonomic considerations and equivalences regarding the *Gephyrocapsa* complex are summarised in Table 3. As *Reticulofenestra asanoi* we consider the Sato and Takayama (1992) general morphology of this taxon but with a maximum diameter longer than 6.5 μm (Wei, 1993).

In the upper part of Core PS2487-6 (after MIS 13), standard calcareous nannofossil events can be used to confirm the MIS identifications. Additionally, other events were calibrated and proposed to improve the stratigraphy in the region.

A well-defined reversal in *Emiliania huxleyi*–*Gephyrocapsa muellerae* was observed at about 30 cm (Figs. 3 and 4a). We believe this to be coincident with the events recorded by Thierstein et al. (1977) in cores V19-240 and V22-174 at MIS 2 and 3. Flores et al. (1997) observed the same event in the Mediterranean cores, estimating an age of 47 kyr (MIS 3). Wells and Okada (1997) reported a similar trend during MIS 2 in DSDP site 594.

The *E. huxleyi* Acme is not well defined in Core PS2487-6. A weak *Gephyrocapsa muellerae*–*E. huxleyi* reversal is observed in MIS 5, but is not comparable with those recorded elsewhere (Thierstein et al., 1977).

MIS 5, especially substage 5e, is characterised in the North Atlantic by a noteworthy peak in *Gephyrocapsa oceanica* (Jordan et al., 1996). In the Pacific Ocean, Wells and Okada (1997) observed peaks in the *E. huxleyi*/medium–large *Gephyrocapsa* ratio at the top of MIS 5. In Core PS2487-6 a relative abundance maximum of this species is observed between 125 and 225 cm (Figs. 3 and 4a). An increase in the relative abundance of *G. muellerae* (*G. muellerae* peak) at the top of MIS 6 together with a sharp reduction during the early MIS 5 agree with the data of Wells and Okada (1997).

During MIS 7 (base) an important decrease is seen in the abundance of *Gephyrocapsa caribbean-*

Table 3
Systematic equivalence of some of the coccolithophore/calcareous nannofossils identified in this study

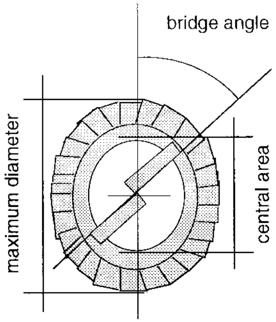

	G. oceanica	*G. muellerae*	*G. caribbeanica*	Small *Gephyrocapsa*	*G. omega*	Large *Gephyrocapsa*
This study						
Bridge angle	>50º	<25º	closed central area	–	∼90º	–
Maximum diameter	>3 μm	>3 μm	>3 μm	<3 μm	>3 μm	>5.5 μm closed central area
Author equivalence						
Bukry (1973)	–	–	–	–	*G. omega*	–
Thierstein et al. (1977)	–	*G. caribbeanica*	–	–	–	–
Bréhéret (1978)	*G. oceanica*	*G. muellerae*	*G. caribbeanica*	*G. aperta* *G. ericsonii*	–	–
Santleben (1980)	*G. oceanica*	*G. muellerae*	*G. caribbeanica*	several species	–	–
Matsuoka and Okada (1990)	*Gephyrocapsa* sp. D (large)	*Gephyrocapsa* sp. D	*Gephyrocapsa* sp. D (small)	*Gephyrocapsa* spp. (small)	*Gephyrocapsa* sp. C	*Gephyrocapsa* sp. B
Sato and Takayama (1992)	–	–	–	–	*G. parallela*	large *Gephyrocapsa*
Raffi et al. (1993)	medium *Gephyrocapsa*	small *Gephyrocapsa*	small *Gephyrocapsa*	small *Gephyrocapsa*	*G. omega*	large *Gephyrocapsa*
Jordan et al. (1996)	*G. oceanica*	*G. muellerae*	–	*G. aperta* *G. ericsonii*	– –	– –
Bollmann (1997)	*Gephyrocapsa* large + equatorial	*Gephyrocapsa* cold	*Gephyrocapsa* oligotrophic	*Gephyrocapsa* minute	– –	– –

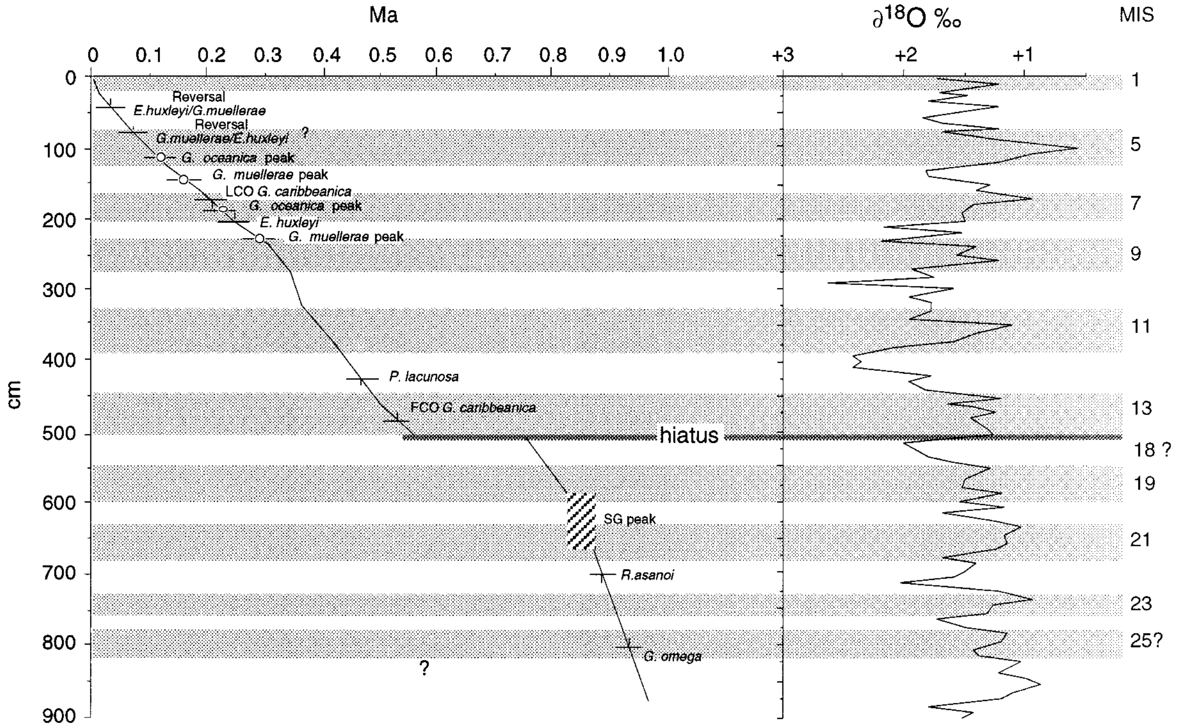

Fig. 3. Estimated sedimentation rates, δ^{18}O isotope curve and location of calcareous nannofossil events in Core PS2487-6. Horizontal grey bars represent the inferred interglacial marine isotope stages (*MIS*).

ica (Last Common Occurrence — LCO) (Figs. 3 and 4a), in agreement with the data of Pujos-Lamy (1977), Pujos and Giraudeau (1993) and Weaver and Thomson (1993). MIS 7, between the LCO of *G. caribbeanica* and the *G. muellerae* peak, is characterised by a peak in small *Gephyrocapsa*, as observed by Weaver and Thomson (1993).

A progressive increase in *G. oceanica* is observed at the base of MIS 8 in Core PS2487-6 (Fig. 4a). In our core, this event coincides with the First Occurrence (FO) of *E. huxleyi*, dated by Thierstein et al. (1977) at 268 kyr (MIS 8). The relative ease with which placoliths of *E. huxleyi* can be dissolved, however, hinders definitive identification of this standard event, especially by light microscopy.

The Last Occurrence (LO) of *Pseudoemiliania lacunosa* is a well-calibrated event at MIS 12 (Thierstein et al., 1977) and well identified in our core. Very close to this event, at the top of MIS 13 the First Common Occurrence (FCO) of *G. caribbeanica* is seen, equivalent to the progressive increase in *Gephyrocapsa* sp. D observed by Matsuoka and Okada (1990) in ODP Site 709.

At about 500 cm a hiatus, coinciding with a sharp contact in the lithology, can be identified (Figs. 2 and 3). The stratigraphy below the hiatus is not so accurate owing to the ambiguous isotopic stratigraphic pattern, and the calcareous nannofossil events identified provide only tentative data. However, a clear reduction in the abundance of *R. asanoi* (a species defined by Sato and Takayama, 1992) is observed at 705 cm, coinciding with relatively high values of δ^{18}O. We interpret this reduction as the LO of *R. asanoi*, which according to Wei (1993) was a relatively synchronous event occurring during MIS 22. Peaks in this nannofossil species recorded during MIS 19 and 18 can be interpreted as reworking. According to this pattern, MIS 20 and 21 are characterised by an increase in the small *Gephyrocapsa* (Figs. 3 and 4b).

Raffi et al. (1993) reported the re-entry of medium-sized *Gephyrocapsa* (mainly *Gephyrocapsa*

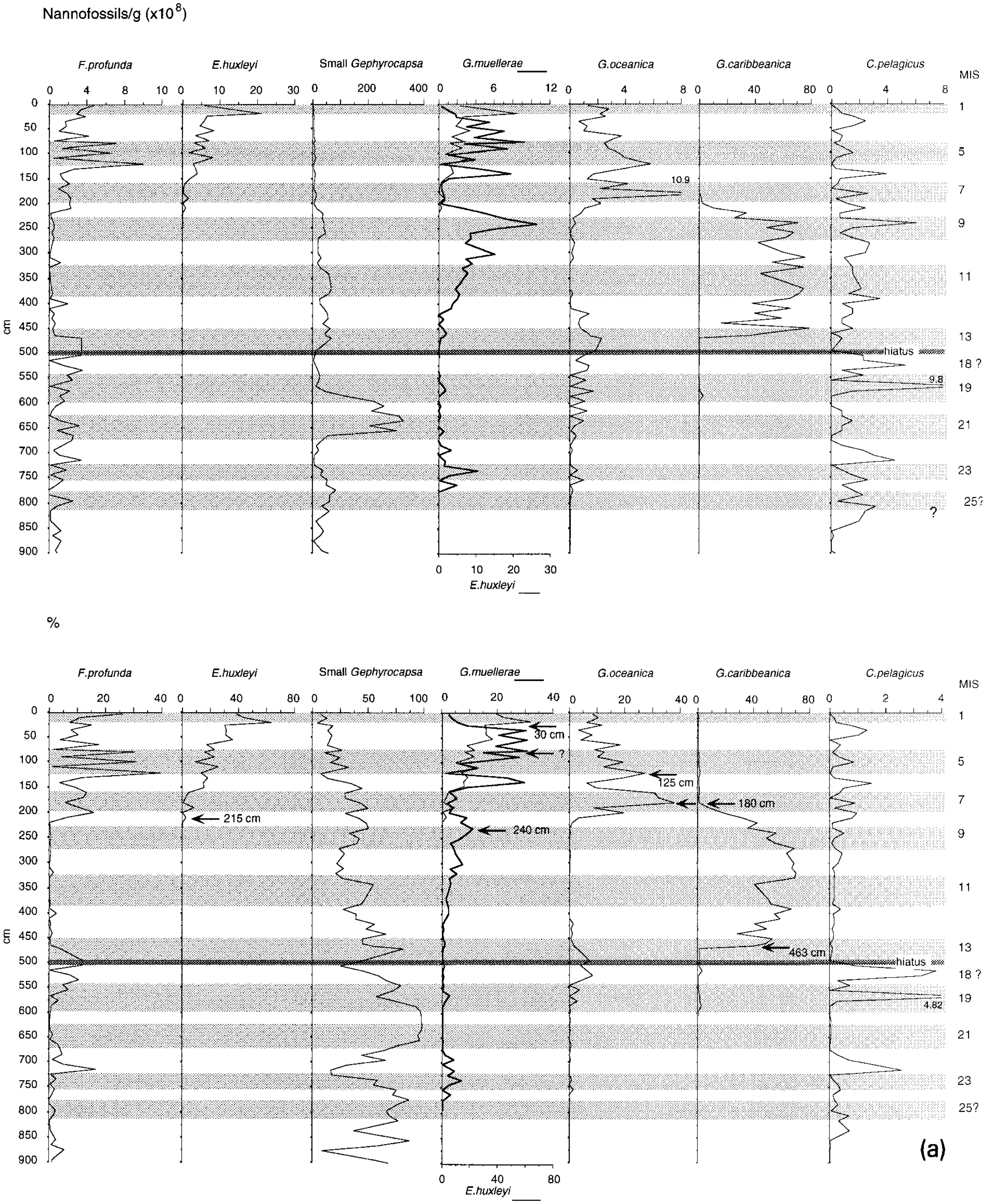

Fig. 4. (a, b) Absolute calcareous nannofossil abundances (nannofossils per g) and percentages in Core PS2487-6 of selected species. Arrows mark the calcareous nannofossil events used for stratigraphy (Fig. 3). Horizontal grey bars represent the inferred interglacial marine isotope stages (*MIS*).

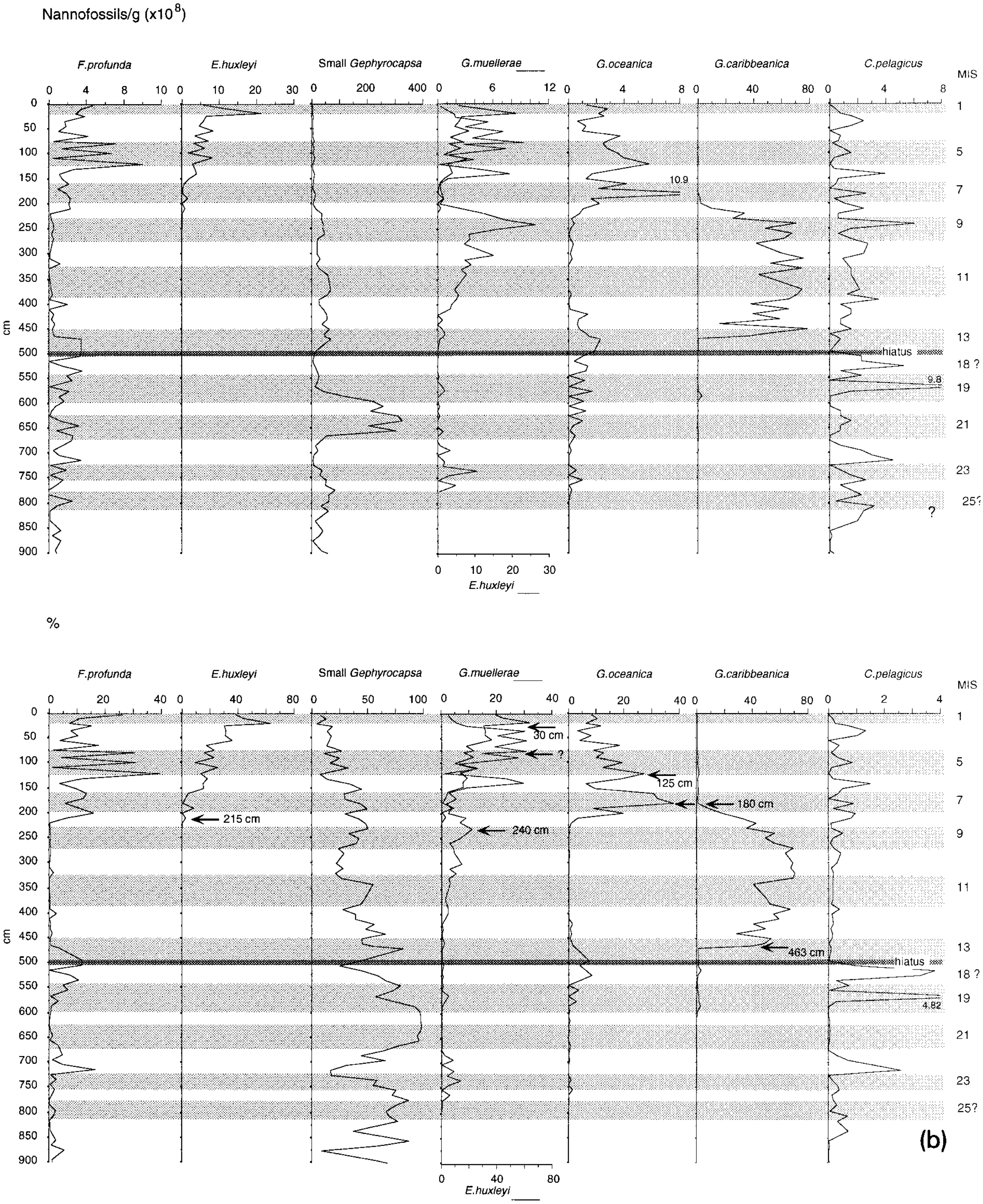

Fig. 4 (continued).

omega) as a diachronous event occurring between IS 25 and 29. The FO of the equivalent morphotypes *Gephyrocapsa* sp. C (Matsuoka and Okada, 1990) has been recorded by Wei (1993) in high latitudes in MIS 25 and 26. In Core PS2487-6, the FO of *G. omega* is recorded at 765 cm, coinciding with low values in the $\delta^{18}O$ record (MIS 25?). Peaks in this species are observed during MIS 23 (Fig. 4b).

5.2. Coccolithophore assemblages in surface sediments

A total of eight surface sediment samples, taken in areas where dissolution does not substantially affect the coccolithophore assemblage, was analysed (Table 1). The results are shown in Fig. 5. The samples come from three main oceanographic regimes: Subtropical (including the AC retroflection area), STCZ and Subantarctic. The nannofossil assemblages from the Subtropical and Subantarctic regimes are significantly different, but intermediate regime samples, such as those from the STCZ, show intermediate characteristics. According to these data, we believe that it should be possible to use the nannofossil assemblages to reconstruct fluctuations between these two oceanographic regimes downcore, at least between MIS 8 and 1, where the coccolithophore record includes the present-day species discussed below.

Two qualitatively and quantitatively different coccolithophore assemblages were distinguished. The subtropical assemblage is characterised by significant proportions of *Florisphaera profunda* (up to 10%), *Gephyrocapsa oceanica* (up to 5%), and *Umbilicosphaera* spp. (up to 1%). The abundances of *F. profunda* and *G. oceanica* decrease from the subtropical to the subantarctic waters (Fig. 5). In the subantarctic assemblage these species are rare or

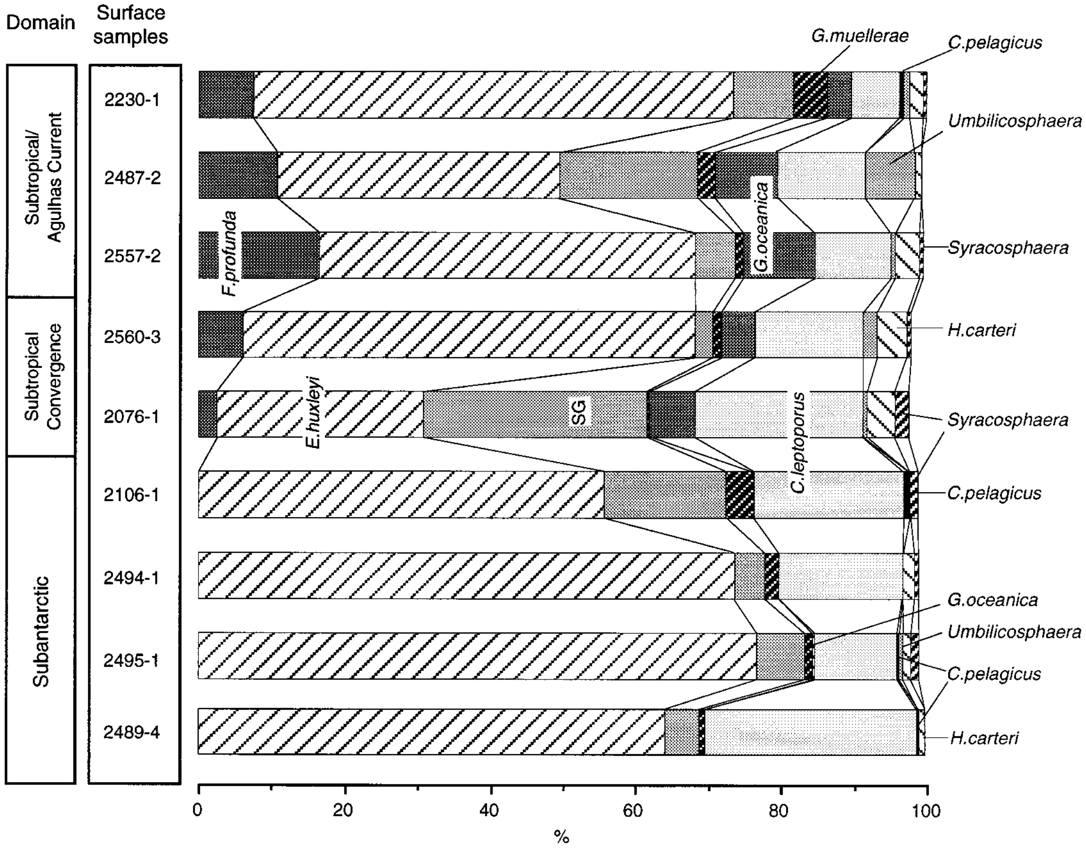

Fig. 5. Coccolithophore abundance in the surface sediment samples studied. Location and sample type in Table 1.

absent. Sample PS2076-1 shows intermediate characteristics, reflecting its position close to the STCZ, with a significant peak in small Gephyrocapsids. Sample PS2560-3 also shows intermediate characteristics, although the assemblage is more similar to those of the subtropical domain assemblages. Other species, such as *E. huxleyi*, *G. muellerae*, and the small *Gephyrocapsa* are also components of the subtropical assemblage although they are also present in subantarctic, subtropical and BC areas. The stratification of the uppermost surface waters from the AC and related eddies, with a moderately deep nutricline, is known to favour *F. profunda* (Molfino and McIntyre, 1990a,b).

5.3. Calcareous nannofossil assemblages

Core sediments contain a variety of nannofossil assemblages. Some of the species considered are extinct. Paleoecological studies of these are very scarce and, in most cases, related to very distant regions. Fortunately, several living species have been recorded regularly in the core. In other cases, we use other proxies that can help to interpret the evolution of the nannofossil assemblages.

Different ‘long-term’ intervals, based on quantitative and qualitative nannofossil constituents, can be distinguished, sometimes coinciding with stratigraphic periods defined by calcareous nannofossils (Fig. 2). Within these intervals, short-term variations linked to the glacial–interglacial cyclicity can also be observed.

The interval from 0 to 200 cm (MIS 1 to 7/8) is characterised by a relatively low abundance of coccoliths and a high concentration of planktonic foraminifera. The weight of foraminiferal calcite ranges between 35 and 65% of the total weight of dry sediment (Fig. 2). The most abundant coccolithophore species are all living taxa, *F. profunda*, *E. huxleyi*, small *Gephyrocapsa* (smaller than 3 μm), *G. oceanica* and *G. muellerae*. Minor proportions of *Calcidiscus leptoporus*, *H. carteri*, *Umbilicosphaera* spp. and *Syracosphaera* spp. are observed. As discussed in the section on stratigraphy, these species vary in their abundances throughout the latest Pleistocene. In general, in this interval *G. oceanica*, *F. profunda*, *Umbilicosphaera* spp. and *Syracosphaera* spp. are observed to covary; the maximum of these taxa coincides with minimum values of $\delta^{18}O$ (interglacial episodes). By contrast, *G. muellerae* follows the opposite trend: the lower part of this interval (MIS 7) is characterised by a peak in *G. oceanica* and a reduction in *G. muellerae*. *Calcidiscus leptoporus* reaches maximum values during interglacial intervals, whereas *Helicosphaera carteri* is relatively more abundant during glacial periods and close to the MIS 7/6 boundary. *Coccolithus pelagicus* is relatively more abundant during glacial periods (Fig. 4a).

The interval from 200 to 450 cm (MIS 7/8 to 13) is characterised by a significant increase in the total abundance of nannofossils, the concentration of planktonic foraminifera decreasing to values between 10 and 40% of the total sample weight (Fig. 2). The most significant feature of this interval is the strong reduction in some stratigraphically long-ranging species such as *F. profunda* and *G. oceanica*. At the same time, *G. caribbeanica* becomes the dominant species together with the small *Gephyrocapsa*. The maximum abundances of small *Gephyrocapsa* coincide with interglacial periods, whereas *G. caribbeanica* shows a weak increase during glacial periods. Other species are recorded in low relative abundances (Fig. 4a).

Between 450 and 575 cm (MIS 13 to 19/20) low abundances of nannofossils similar to those observed in the uppermost interval are observed. The percentage of foraminiferal calcite varies between 35 and 70% of the total sample weight (Fig. 2). A more diverse assemblage is mainly dominated by small *Gephyrocapsa*, *P. lacunosa* and *F. profunda*, and peaks in *G. oceanica* and *Umbilicosphaera* spp., are observed. *Gephyrocapsa caribbeanica* shows a strong reduction in the lower part of this interval. *Coccolithus pelagicus* and *H. carteri* show peaks in MIS 18 (?) and 19. These peaks coincide with the minimum values of *F. profunda*.

A hiatus is interpreted at 500 cm (Figs. 2 and 3). A positive correlation between *F. profunda*, *G. oceanica*, *Umbilicosphaera* spp., *P. lacunosa* and *C. leptoporus* is observed in this interval.

From 575 to 650 cm (MIS 19/20 to 21/22) an important increase in the abundance of nannoliths is seen due to a peak in small *Gephyrocapsa*. Other species are less abundant, with a weak peak in *H. carteri*, *C. leptoporus* and *C. pelagicus* during MIS 21.

As mentioned above, below 670 cm (below MIS 18) the isotope stratigraphy is not totally reliable and the data must be considered as tentative. The nannofossil assemblages are dominated by the small *Gephyrocapsa* as well as *P. lacunosa* and *C. leptoporus*. In these species, no clear relationship between abundance and the glacial–interglacial pattern is observed. *Florisphaera profunda* and *C. pelagicus* show sporadic peaks, also inconsistent with the glacial–interglacial pattern (Fig. 4a and b).

5.4. Planktonic foraminifera

Three different assemblages are abundant in Core PS2487-6. *Globorotalia inflata* is a species characteristic of the transition zone lying between the subtropical and subantarctic waters (Bé and Tolderlund, 1971; Bé, 1977). Today, the assemblage dominated by *G. inflata* is usually abundant north of the STCZ while *Globigerina bulloides* and *Neogloboquadrina pachyderma* (dextral) are dominant south of the STCZ (Hutson, 1980). *Globigerina bulloides* and *N. pachyderma* are also abundant along the Southwest African continental margin in the intermediate zone of the Benguela system, where upwelled eutrophic and offshore oligotrophic waters mix. Additionally, *Globigerinoides ruber* is not abundant in the South Atlantic at this latitude; the highest percentages of this species south of Cape Town are today clearly linked to the influence of the tropical waters of the AC retroflection.

Cold-eutrophic foraminifera (*G. bulloides*, *Neogloboquadrina pachyderma* and *Turborotalita quinqueloba*) with values of around 60% of the total assemblage are the most abundant group in the core. *Globorotalia inflata* is also abundant between MIS 1 and 9, its abundance being reduced from MIS 9 to MIS 13. The tropical species (*G. ruber* along with a low proportion of *Globigerinoides sacculifer*) persist with low values (around 5%) during glacials but increase sharply (20%) during major deglaciations (terminations I, II, and V). This incursion of tropical forms was not observed at Termination III, although this could be due to sampling resolution. The tropical faunas are abundant only during a short period following each deglaciation. A remarkable quantitative change in the planktonic foraminifera can be identified at the limit between MIS 11 and 12, defined by an abrupt increase downcore in the species characteristic of subantarctic and Antarctic waters. *Neogloboquadrina pachyderma* (sinistral), a typical form of Antarctic waters or the extremely eutrophic waters of the Benguela system, is almost absent until MIS 12, where it increases to reach values above 10% of the total assemblage. Additionally, the tropical and subtropical foraminifera reach the minimum values (2%) during MIS 12.

From the hiatus downwards, the general pattern is very similar; the cold eutrophic foraminifera are more abundant during MIS 18 (?), characterised by lower values of *G. inflata*, while between MIS 20 and 21 the opposite trend can be recognised. From MIS 22 and 23 the cold-eutrophic foraminifera are again replaced by *G. inflata*. During glacials below the hiatus, *G. ruber* and *G. sacculifer* are recorded with mean values higher that those obtained in the upper part. As seen above, strong influxes of these species seem to occur at the base of major interglacials (MIS 19, 21 and 23) (Fig. 6).

6. Discussion

6.1. Coccolithophores and calcareous nannofossils as paleoceanographic indicators

6.1.1. Assemblages

Core PS2487-6 comes from an area influenced by the AC, where anticyclonic eddies begin their displacement northwards into the Atlantic Ocean (Lutjeharms, 1981; Lutjeharms and Meeuwis, 1986; Schumann, 1987; Shannon et al., 1990). Since the AC and subantarctic coccolithophore assemblages differ in their composition they can help to monitor the evolution of these water masses in a given area. The few studies on coccolithophores in surface and downcore sediments related to the AC reveal a dominance of *E. huxleyi*, *G. oceanica*, *C. leptoporus* and *Umbilicosphaera sibogae*, with percentages similar to those seen in this study (Fincham and Winter, 1989; Winter and Martin, 1990). Studies on living coccolithophores have yielded similar results: *E. huxleyi* and *G. oceanica* are the most abundant species, whereas south and east of the AC *Umbilicosphaera hulburtiana* and *Umbellosphera tenuis* are dominant (Friedinger and Winter,

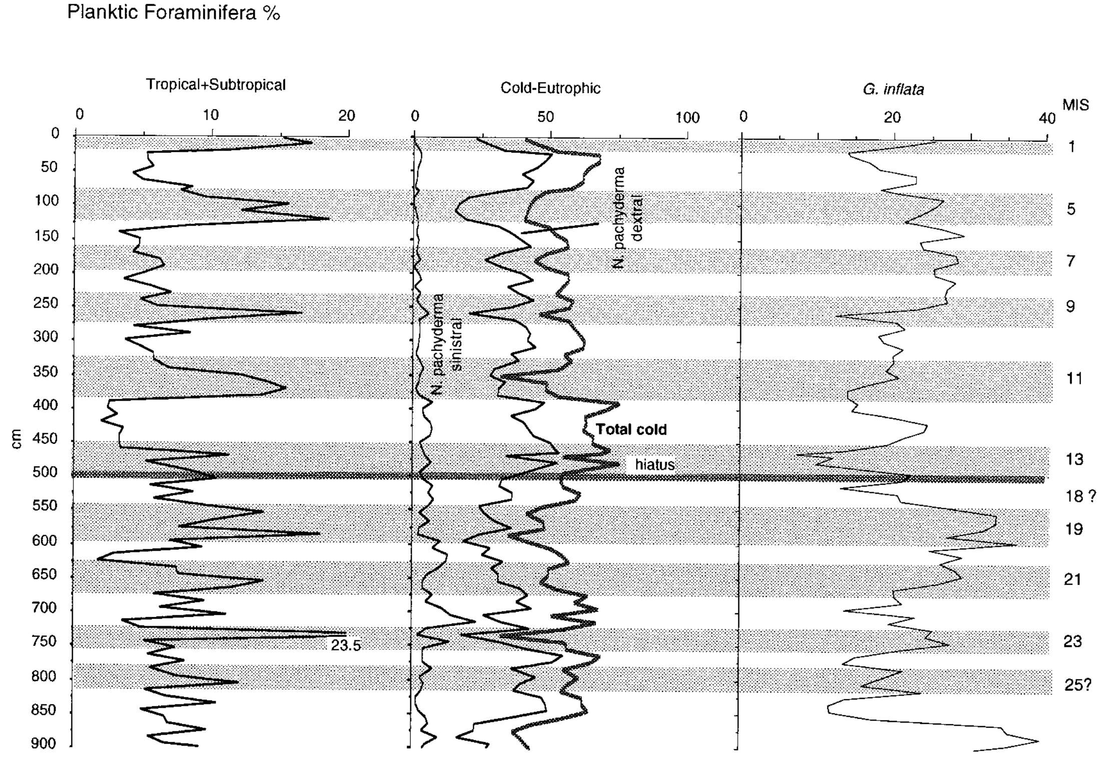

Fig. 6. Relative abundance (percentages) of planktonic foraminifera groups. The Cold-Eutrophic planktonic foraminifera group include *G. bulloides*, *N. pachyderma* and *T. quinqueloba*. The Tropical + Subtropical group include *G. ruber* (dominant) and *G. sacculifer*. For details see text and Appendix A. Horizontal grey bars represent the inferred interglacial marine isotope stages (*MIS*).

1987). Giraudeau (1992) observed that today the BC coccolithophore assemblages mainly consist of *G. oceanica*, *H. carteri*, *C. leptoporus*, *C. pelagicus*, *Syracosphaera* spp., *Rhabdosphaera* spp., *U. sibogae*, and the calcareous dinoflagellate *Thoracosphaera* spp., although the dominant taxa are *E. huxleyi* and small *Gephyrocapsa*. These species are frequent in our core and, according to our observations, the coccolithophore assemblage is not affected by dissolution. In DSDP Site 594 (south of New Zealand, in the STCZ), for the last five MIS Wells and Okada (1997) reported an assemblage formed by *E. huxleyi*, small- and medium-sized *Gephyrocapsa* and *Reticulofenestra*, and minor proportions of *H. carteri*, *C. pelagicus*, *Syracosphaera* and *C. leptoporus*. In ODP Hole 704A (Southern Atlantic Ocean, Subantarctic surface water) Gard and Crux (1991) observed a dominance of placoliths <2.5 μm during the last thirteen MIS.

From the qualitative point of view, these data do not point to clear differences between the AC, BC, or subtropical coccolithophore assemblages. Only the subantarctic assemblage is characterised by the absence of *F. profunda* and low proportions of *G. oceanica* and *Umbilicosphaera* spp.; this is supported by our results on surface sample analysis (Fig. 5).

In our core, species linked to the Upper Photic Zone (UPZ) and/or Middle Photic Zone in stratified waters, such as *Ceratolithus* spp., *Umbellosphaera* spp., *Neosphaera coccolithomorpha*, or *Rhabdosphaera* spp. (Jordan et al., 1996; Jordan and Chamberlain, 1997), occur in very low proportions. Only *Syracosphaera* s.l., linked to these upper and middle photic layers (Jordan and Chamberlain, 1997), shows maximum values above MIS 8, with a similar trend to that of *F. profunda*. Other abundant species in Core PS 2487, such as *E. huxleyi*, *Gephy-*

rocapsa spp., *Helicosphaera* spp. either have no depth preference or live mainly in the UPZ (Okada and McIntyre, 1977, 1979; Molfino and McIntyre, 1990a,b; Jordan and Chamberlain, 1997).

6.1.2. Notes on individual species

Florisphaera profunda is a Lower Photic Zone (LPZ) inhabitant which occurs above the 12ºC isotherm and is clearly related to nutricline dynamics (Okada and Honjo, 1973; Okada, 1980; Molfino and McIntyre, 1990a,b). This species avoids shallow thermoclines and strong light levels (Ziveri et al., 1995). The ratio between *F. profunda* and other coccolithophores has been proposed as a tool for estimating the relative position of the nutricline in time and space (Molfino and McIntyre, 1990a,b). No data for the *F. profunda* record have been reported in the region studied. According to our data, this organism is common in the AC environment, with values of 8–15% (Fig. 5), although no information on the position of the nutricline is available.

In core PS2487-6 peaks in *F. profunda* are observed during MIS 1, 5 and 7 (Fig. 4a). However, below MIS 8 the increase that occurred during interglacial intervals is not observed. This is coincident with a major downcore increase in *G. caribbeanica*, which in older sediments is the dominant taxon. Likewise, *G. caribbeanica*, morphologically equivalent to Bollmann's (1997) *Gephyrocapsa* 'oligotrophic', starts in a cold interval (transition to the cold MIS 12) and has its LCO at the beginning of MIS 7, although coinciding with a warm period. Consequently, for the interval corresponding to MIS 9 to 12 the Molfino and McIntyre (1990a,b) model does not seem to be useful.

Gephyrocapsa oceanica is widely reported as a warm water species with a preference for marginal seas (McIntyre and Bé, 1967; Okada and Honjo, 1975; Jordan et al., 1996). Winter (1982) and Winter and Martin (1990) linked *G. oceanica* to high fertility and neritic environments and concluded that for the AC region peaks in this species are related to high productivity pulses. This interpretation is supported by the studies of Ziveri et al. (1995) in the Gulf of California. Giraudeau (1992) observed in the BC area that *G. oceanica* is linked to relatively warm, high nutrient content surface waters; it is scarce in cold, fertile waters. Prell et al. (1980) link this species to the AC tropical waters. In our core we observed a parallel distribution between *G. oceanica* and *F. profunda* and conclude that these species may be controlled by the same ecological factors (or at least one factor). In our core, maximum values are recorded during MIS 7, and close to terminations II and I.

Calcidiscus leptoporus is a controversial species. Jordan et al. (1996) observed a negative correlation between the presence of this species and temperature. Giraudeau (1992) observed a progressive increase in upwelling cells off west Africa. Winter (1982), and Fincham and Winter (1989) correlate the abundance of *C. leptoporus* with increases in water fertility in the Red Sea and Indian Ocean. However, other authors link the abundance of this species with oligotrophic conditions (Blasco et al., 1980) and it is not reported in other upwelling regions (Mitchel-Innes and Winter, 1987). Gard and Crux (1991) observed peaks in this species during MIS 1, 5, 7 and 13, in agreement with an increase in temperature and a southward displacement of the Antarctic Convergence Zone. In the Pleistocene sediments from South Australia, Wells and Okada (1996) linked relatively high proportions of *C. leptoporus* with warm (interglacial) conditions. In our core, the maximum abundance of *C. leptoporus* is observed at the beginning of deglaciation, with marked peaks during MIS 1 and 5 (terminations I and II).

Helicosphaera carteri is a cosmopolitan species with a temperature range in present day water masses from 5 to 30ºC, but with an optimum temperature of 21ºC (McIntyre and Bé, 1967; Okada and McIntyre, 1979; Mostajo, 1985). Estrada (1978) and Giraudeau (1992) observed this species in relatively high abundances in upwelling regions. Similarly, Pujos (1992) and Flores et al. (1995) correlated the highest values with high productivity episodes in Plio-Pleistocene sediments. In Core PS2487-6, the most significant peaks in *H. carteri* are observed during glacial periods 2 to 4 (Fig. 4b).

Coccolithus pelagicus is a traditional cold water indicator, ranging from 7 to 14ºC, with an optimum of 8 to 10ºC (McIntyre and Bé, 1967; McIntyre et al., 1970). More recent data have extended the range of this 'classical' marker (e.g. Blasco et al., 1980). Giraudeau (1992) correlated the abundance of this species with cold conditions in upwelling cells, and Cachão and Moita (1995) reported the presence of this species linked to upwelling cells in the Portuguese upwelling. In our core, a weak correlation with the δ^{18}O curve can be found. However, an inverse correlation with *F. profunda* is observed, although the maximum abundance of *C. pelagicus* is recorded in the intervals where *F. profunda* is abundant. Also, peaks in *C. pelagicus* correspond to maximum values of δ^{18}O (glacial periods), with the exception of MIS 19 and 9.

Gephyrocapsa muellerae is a cold Atlantic species (Jordan et al., 1996; Flores et al., 1997) equivalent to the *Gephyrocapsa* 'cold' morphotype described by Bollmann (1997). In our core, a clear relationship between the increase in its percentages and glacial periods can be seen during the time in which this species became dominant. Reduced abundances were especially pronounced during deglaciations (Fig. 4a).

In the North Atlantic, *G. caribbeanica* is a species that is especially abundant below MIS 7 (Weaver and Thomson, 1993; Flores, in Villanueva, 1996). Wells and Okada (1997) link this species with *C. pelagicus*, suggesting a relationship with cold conditions. In our core, a clear correlation with glacial intervals is observed in the interval of maximum abundance, although few specimens are found after MIS 7. Nishida (1986) reported that this species was most abundant between the STCZ and Subantarctic Front (linked to Subantarctic water masses). However, this species is considered equivalent to the *Gephyrocapsa* 'oligotrophic' by Bollmann (1997), characteristic of gyre areas. During the Mid-Brunhes interval, where high temperatures characterised MIS 7 and 11 in the Southern Hemisphere (Jansen et al., 1986; Hodell, 1993), maximum values of *C. caribbeanica* are recorded, although with minimum values during the glacial intervals. The abundance of this species increases dramatically at the top of MIS 13, close to MIS 12, and declines close to Termination III (Fig. 4a). The significance of this species in our core is not well understood. Its bloom during the Mid-Brunhes seems to be an evolutionary response rather than an ecological one. A strong reduction in *F. profunda* during a warm period is not consistent with the increase in another species (i.e. *C. caribbeania*) when both are thought to be indicative of oligotrophic waters.

The small *Gephyrocapsa* group (Table 3) is one of the most abundant (Fig. 4a). Together with *E. huxleyi*, this group is considered by Wells and Okada (1997) as an 'upwelling' indicator. In our core, maximum values of both taxa are observed during interglacial periods, with a very sharp peak recorded during MIS 19 to 21. However, an opposite trend between these taxa and the cold-eutrophic planktonic foraminifera studied may be observed (Fig. 4a and Fig. 6). The abundance both of *E. huxleyi* and small *Gephyrocapsa* here seems to be linked to paleotemperature (STCZ displacement, as we discuss in next section) rather than nutrient content.

Syracosphaera spp. is a complex group that is poorly understood from the ecological point of view. Estrada (1978) and Giraudeau (1992) found high concentrations of this taxon in highly productive areas. Jordan et al. (1996) reported that this group tends to be more abundant and diverse in subtropical waters and observed a relatively low proportion in Holocene sediments from the western African upwelling, which could be related to a preference for warm and stratified waters. Other authors have linked the abundance of this species to low salinity conditions, although a warm water component has also been suggested (Weaver, 1983). In our samples, *Syracosphaera pulchra* is the most important species of the genus. According to our data, here *Syracosphaera* is a warm water indicator, showing maximum abundances during interglacial periods, with significant peaks during deglaciations (especially terminations V, IV and I; Fig. 4b).

Umbilicosphaera sibogae has been reported as being present in many oceans, with a temperature range between 18 and 24ºC (McIntyre and Bé, 1967; Okada and McIntyre, 1979), and as an inhabitant of medium-to-high fertility regions (Roth and Berger, 1975). Giraudeau (1992) observed a similar distribution between *C. leptoporus* and *U. sibogae* and therefore considers *U. sibogae* as an oligotrophic indicator. Wells and Okada (1996) considered *U. sibogae* to be a tropical form. Fincham and Winter (1989) recorded this species in surface sediments from the AC retroflection region at abundances of around 10%. We also note that other species, such as *Gephyrocapsa oceanica*, show a similar pattern to *U. sibogae*. In our core and surface sediment samples, the abundance of *U. sibogae* is similar to that of *F. profunda* and *G. oceanica*, showing peaks during interglacial periods, but especially during terminations V, IV, III, II and I (Fig. 4a and b).

6.2. Paleoceanography

Core PS2487-6 is situated in the zone of influence of the AC with a warm, well-stratified water nannofossil assemblage during the Holocene. The evolution of coccolithophore and planktonic foraminifera allows us to clearly trace the short-term, glacial–interglacial cyclicity between MIS 1 to 8.

Several authors have suggested changes of less than 5° northwards in the position of the STCZ during cold (glacial) periods and little variation in the southern boundary of central gyres (Prell et al., 1979; Morley and Hays, 1979; Niebler, 1995). In general, it has been established that the STCZ lay south of 42°S during MIS 7, 9 and 11, with short poleward excursions also during the early part of MIS 1 and 5 (Prell et al., 1979; Howard and Prell, 1992). These rapid, short STCZ excursions coincided with the increase in tropical and subtropical calcareous plankton seen in this study, especially during terminations (Fig. 4a, b and Fig. 6). The prominent incursions of tropical and subtropical foraminifera (mainly *G. ruber*, a species today linked to the AC) seem to indicate a clear influence of these warm waters during these periods (Fig. 6). Hutson (1980) and Prell et al. (1980) have reported that during cold periods the AC decreased in intensity, becoming cooler, shallower and showing a greater seasonality. In our core, during glacial MIS 2-4, 6 and 8 the calcareous nannofossil assemblages, characterised by a relative reduction in *F. profunda* and increase of *Gephyrocapsa* spp. and *E. huxleyi*, indicate an intense mixing and rising of the nutricline (Fig. 4a), probably linked to a northwards displacement of the STCZ and an eastward movement of the AC retroflection. The strong abundance of cold-eutrophic foraminifera (Fig. 6) during the same glacial stages together with the low percentages of tropical and subtropical planktonic foraminiferal clearly support this idea. The reduction in subtropical coccolithophore species in some intervals during MIS 5 could correspond to cold substages, although poor resolution prevents a precise interpretation.

In any case, the record of subtropical species, although in low proportions, allows us to interpret that during cold MIS 2–4, 6 and 8 the area was close to the STCZ, but never directly influenced by subantarctic surface waters and indicates that the AC retroflection had not collapsed.

As noted in the previous section, a dramatic change in the calcareous nannofossil assemblage is observed during the interval from MIS 8 to 12, just at the top of the MIS 13 warm period. A strong reduction (both absolute and relative, Fig. 4a) can be observed in *F. profunda* and *G. oceanica*. These species, linked to the warm AC in surface sediment samples, are very rare even during MIS 9 and 11. However, the increases in tropical and subtropical planktonic foraminifera and in *C. leptoporus*, *Umbilicosphaera* spp. and *Syracosphaera* spp. during these stages agree with an enhanced subtropical and AC influence. *Gephyrocapsa caribbeanica*, an oligotrophic (subtropical?) species (sensu Bollmann, 1997), is the dominant calcareous nannofossil taxon in this interval. However, as discussed previously it is not easy to distinguish the ecological and evolutionary effects here. According to Hodell (1993), who studied ODP Hole 704A, MIS 9 and 11 had the lowest $\delta^{18}O$ values of the 3.2 Ma, indicating unusually high temperatures and a very southerly position of the PFZ in the Southern Atlantic Ocean. These data coincide with a high coccolithophore (and calcium carbonate) concentration (Gard and Crux, 1991). The southward displacement of the PFZ must have been accompanied by a northward STCZ displacement (Howard and Prell, 1992; Hodell, 1993). Although we cannot confirm a major increase in temperature during MIS 9 and 11, the different concentrations and compositions of the calcareous plankton assemblages could reflect some paleoceanographic change not yet understood but linked to the Mid-Brunhes event. Jansen et al. (1986) reported an intensified atmospheric and oceanic circulation in the Southern Hemisphere during that time, linked to a perturbation due to the orbital eccentricity cycle of 413 kyr.

Between MIS 11 and 12 the sharp increase downcore in the cold eutrophic foraminifera, including *N. pachyderma* sinistral, and the reduction in the subtropical forms both in planktonic foraminifera and calcareous nannofossils have been related to a northward displacement of the PFZ and STCZ (Hodell, 1993). The flora and fauna recorded in MIS 12 suggest that this was one of the coldest episodes in the Pleistocene.

The interpretation of the interval defined below the hiatus (Figs. 2 and 3) is less accurate owing to poorer stratigraphic resolution. Small *Gephyrocapsa* are the dominant group in this interval. This group is considered an upwelling (eutrophic?) morphotype (Wells and Okada, 1997); consequently, the noteworthy peak observed during MIS 19 to 21 could be interpreted as a high productivity peak in the area studied. The dramatic reduction in *F. profunda* in this interval supports this interpretation. However, the reduction in the cold-eutrophic foraminifera and the increase in *G. inflata* do not agree with the calcareous nannofossil interpretation. Conversely, MIS 22 (apparently dominated by warm-oligotrophic calcareous nannofossils) is characterised by high values of cold-eutrophic foraminifera. Other proxies will be necessary to better understand environmental conditions during these intervals.

7. Conclusions

Several bioevents previously observed in medium and low latitudes have been identified and calibrated with the δ^{18}O isotope curve. The high degree of synchronicity between these events and those observed in the North Atlantic and Indian oceans is noteworthy. A reversal between *E. huxleyi* and *G. muellerae* is observed in Marine Isotope Stage (MIS) 2 to 4. A peak in the abundance of small *Gephyrocapsa* is correlated with MIS 7, synchronous with a dramatic reduction in the abundance of *G. caribbeanica*. The reduction in this species starts close to the FO of *E. huxleyi*. The FCO of *G. caribbeanica* is observed at the top of MIS 13 and coincides with a reduction in *P. lacunosa* specimens, which have their LO in MIS 12. The LO of *R. asanoi* and the FCO of *G. omega* are tentatively placed in MIS 22 and 25, respectively, immediately after a sharp increase in small *Gephyrocapsa* during MIS 19 to 21.

The interval of dominance of *G. caribbeanica* dates the warm episode of the so-called Mid-Brunhes event (MIS 7 to 11), characterised in the Southern Ocean by an increase in $CaCO_3$.

Study of surface sediment samples in the region allows us to identify a typical assemblage characterising the Agulhas Current (AC). This assemblage indicates warm, stratified waters. The model is useful to interpret the interval from MIS 1 to 8, and the interval below MIS 11. The episode from MIS 8 to 12 has an assemblage dominated by *G. caribbeanica*, with a reduction in the subtropical species linked to the AC. The ecological interpretation of this species is controversial due to an evolutionary overprint. However, during the dominance interval, maximum values of this species are recorded in the glacial MIS 12 and 10.

During the interval studied, glacial–interglacial cyclicity is well defined in the AC retroflection area (Core PS2487-6). This glacial–interglacial cyclicity responds to a fluctuation in the STCZ, probably linked to an eastward and westward displacement of the AC retroflection. In any case, the core studied was always under subtropical conditions, with an enhanced influence of the AC during interglacial periods. For the whole interval, the increase in *C. leptoporus*, *Umbilicosphaera* spp., *Syracosphaera* spp. and *G. ruber* corresponds to interglacial pulses, maximum values being close to or coinciding with deglaciations.

During some glacial stages, such as MIS 12, we interpret intense cold conditions linked to a northward displacement of the STCZ, although the influence of the AC retroflection was always present.

Acknowledgements

The authors wish to express thanks to Dr. Adolfo Molina (Universidad Nacional Autónoma, Mexico) for his valuable suggestions and critical comments on this study and to N.S.D. Skinner and Claire Findlay for revising the English version of the MS. We also appreciate the comments and suggestions of Jeremy Young (The Natural History Museum, London), Patricia Wells, Jaques Giraudeau (Université de Bourdeaux), and an anonymous reviewer who contributed to improving the original manuscript. Isotope measurements have been accomplished in the AWI isotope laboratory under the helpful guidance of Dr. A. Mackensen. Jesús Roncero is also thanked for his help in sample processing. Research grant CICYT ANT94-0277, CL98-1002-CO2-02 and the Spain–German Acciones Integradas supported this study. This study is the AWI contribution No. 1568 and the SFB contribution No. 267.

Appendix A. Taxonomic appendix

Calcareous nannofossils

Calcidiscus leptoporus (Murray and Blackman, 1898) Loeblich and Tappan, 1978
Coccolithus pelagicus (Wallich, 1877) Schiller, 1930
Emiliania huxleyi (Lohmann, 1902) Hay and Mohler in Hay et al., 1967
Florisphaera profunda Okada and Honjo, 1973
Gephyrocapsa aperta Kamptner, 1963
Gephyrocapsa caribbeanica Boudreaux and Hay, 1967
Gephyrocapsa ericsonii McIntyre and Bé, 1967
Gephyrocapsa muellerae Bréhéret, 1978
Gephyrocapsa oceanica Kamptner, 1943
Gephyrocapsa omega Bukry, 1973
Helicosphaera carteri (Wallich, 1877) Kamptner, 1954
Neosphaera coccolithomorpha Lecal-Schlauder, 1950
Pseudoemiliania lacunosa (Kamptner, 1963) Gartner, 1969
Reticulofenestra asanoi Sato and Takayama, 1992
Syracosphaera pulchra Lohmann, 1902
Umbilicosphaera sibogae (Weber-van Bosse, 1901) Gaarder, 1970
Umbilicosphaera hulburtiana Gaarder, 1970
Umbellosphera tenuis (Kamptner, 1937) Paasche, in Markali and Paasche, 1955

Planktonic foraminifera

Globigerina bulloides d'Orbigny, 1826
Turborotalita quinqueloba (Natland, 1938)
Neogloboquadrina pachyderma (Ehrenberg, 1861)
Globigerinoides ruber (d'Orbigny, 1839)
Globorotalia inflata (d'Orbigny, 1839)
Globigerinoides sacculifer (Brady, 1877)

References

Bé, A.W.H., 1977. An ecological, zoogeographic and taxonomic review of recent planktonic foraminifera. In: Ramsay, A.T.S. (Ed.), Oceanic Micropaleontology. Academic Press, London, Vol. 1, pp. 1–100.

Bé, A.W.H., Duplessy, J.C., 1976. Subtropical convergence fluctuations and Quaternary climates in the middle latitudes of the Indian Ocean. Science 194, 419–422.

Bé, A.W.H., Tolderlund, D.S., 1971. Distribution and ecology of living planktonic foraminifera in surface waters of the Atlantic and Indian Oceans. In Funnel, B.M., Riedel, W.R. (Eds.), The Micropaleontology of Oceans. Cambridge Univ. Press, pp. 105–149.

Blasco, D., Estrada, M., Jones, B., 1980. Relationship between the phytoplankton distribution and composition and the hydrography in the Northwest African upwelling region near Cabo Corbeiro. Deep-Sea Res. 27, 799–819.

Bolli, H.M., Ryan, W.B.F. et al., 1978. Init. Rep. DSDP 40.

Bollmann, J., 1997. Morphology and biogeography of the genus *Gephyrocapsa* coccoliths, in Holocene sediments. Mar. Micropaleontol. 29, 319–350.

Bréhéret, J.G., 1978. Formes nouvelles quaternaires et actuelles de la famille Gephyrocapsaceae (Coccolithophorides). C.R. Acad. Sci. Paris Ser. D 287, 447–449.

Broecker, W.S., 1987. The biggest chill. Nat. Hist. Mag. 97, 74–82.

Broecker, W.S., 1991. The Great Ocean Conveyor. Oceanography 4, 79–89.

Bukry, D., 1973. Coccolith stratigraphy — eastern equatorial Pacific, Leg 116 Deep Sea Drilling Project. Init. Rep. Deep Sea Drill. Proj. 16, 653–712.

Cachão, M., Moita, M.T., 1995. *Coccolithus pelagicus*, a sort of productivity proxy? 6th Int. Nannoplankton Conference, Copenhagen, pp. 33–34 (abstract).

Chapman, P., Duncombe Rae, C.M., Allanson, B.R., 1987. Nutrients, chlorophyll and oxygen relationships in the surface layers at the Agulhas Retroflection. Deep-Sea Res. 34 (8A), 1399–1416.

Estrada, M., 1978. Mesoscale heterogeneities of the phytoplankton distribution In: Boje, R., Tomczak, M. (Eds.), The Upwelling Region of North West Africa. (Upwelling Ecosystems.) Springer, Berlin, pp. 15–23.

Fincham, M., Winter, A., 1989. Late Quaternary paleoceanography of the Southwest Indian Ocean. Mar. Micropaleontol. 13, 325–351.

Flores, J.A., Sierro, F.J., 1997. Revised technique for calculation of calcareous nannofossil accumulation rates. Micropaleontology 43, 321–324.

Flores, J.A., Sierro, F.J., Raffi, I., 1995. Evolution of the calcareous nannofossil assemblage as a response to the paleoceanographic changes in the Eastern equatorial Pacific from 4 to 2 Ma (Leg 138, Sites 849 and 852). Proc. ODP Init. Rep. 138, 163–176.

Flores, J.A., Sierro, F.J., Francés, G., Vázquez, A., Zamarreño, I., 1997. The last 100,000 years in the western Mediterranean: sea surface water and frontal dynamics as revealed by coccolithophores. Mar. Micropaleontol. 29, 351–366.

Friedinger, P., Winter, A., 1987. Distribution of modern coccolithophore assemblages in the area of the Natal Valley (Southwest Indian Ocean). J. Micropalaeontol. 6, 49–56.

Fu, L.L., 1996. The circulation and its variability of the South Atlantic Ocean: first results from the TOPEX/POSEIDON mission. In: Wefer, G. et al. (Eds.), The South Atlantic: Present and Past Circulation. Springer, Berlin, pp. 63–82.

Gard, G., Crux, J., 1991. Preliminary results from Hole 704A: Arctic–Antarctic correlation through nannofossil biochronology. Proc. ODP Sci. Results 114, 193–200.

Gersonde, R. et al., 1995. The Expedition ANTARKTIS-XI/2 of RV 'Polarstern', in 1993/94. Ber. Polarforsch. 163, 1–133.

Giraudeau, J., 1992. Distribution of Recent nannofossils beneath the Benguela system: Southwest African continental margin. Mar. Geol. 108, 219–237.

Giraudeau, J., 1993. Planktonic foraminiferal assemblages in surface sediments from Southwest African continental margin. Mar. Geol. 110, 47–62.

Gordon, A.L.J., 1986. Interocean exchange of thermocline water. J. Geophys. Res. 91, 5037–5046.

Gordon, A.L.J., Lutjeharms, J.R.E., Gründlingh, M.L., 1987. Stratification and circulation at the Agulhas Retroflection. Deep-Sea Res. 34 (4), 565–599.

Gordon, A.L., Weiss, R.F., Smethie, W.M., Warner, M.J., 1992. Thermocline and Intermediate water communication between the South Atlantic and Indian oceans. J. Geophys. Res. 97 (5), 7232–7240.

Gründlingh, M.L., 1985. Features of the circulation in the Mozambique Basin in 1981. J. Mar. Res. 43, 779–792.

Gründlingh, M.L., 1986. Features of the northern Agulhas Current in spring. S. Afr. J. Sci. 82, 18–20.

Hodell, D.A., 1993. Late Pleistocene paleoceanography of the South Atlantic sector of the Southern Ocean: Ocean Drilling Program Hole 704A. Paleoceanography 8, 47–67.

Howard, W.R., Prell, W.L., 1992. Late Quaternary surface circulation of the southern Indian Ocean and its relationship to orbital variations. Paleoceanography 7, 79–117.

Hut, G., 1987. Stable isotope reference samples for geochemical and hydrological investigations. Report to the Director General, International Atomic Energy Agency, Vienna, Sept. 16–18, 42 pp.

Hutson, W.H., 1980. The Agulhas Current during the Late Pleistocene, analysis of modern faunal analogues. Science 207, 64–66.

Jansen, J.H.F., Kuijpers, A., Troelstra, S.R., 1986. A Mid-Brunhes climatic event: long-term changes in global atmosphere and ocean circulation. Science 233, 619–622.

Jordan, R.W., Chamberlain, A.H.L., 1997. Biodiversity among Haptophyte algae. Biodivers. Conserv. 6, 131–152.

Jordan, R.W., Zhao, M., Eglinton, G., Weaver, P.P.E., 1996. Coccolith and alkenone stratigraphy and palaeoceanography at an upwelling site off NW Africa (ODP 658C) during the last 130,000 years. In: Whatley, R., Moguilevsky, A. (Eds.), Microfossils and Oceanic Environments. Univ. Wales, Aberystwyth Press, Aberystwyth, pp. 111–130.

Lutjeharms, J.R.E., 1981. Spatial scales and intensities of circulation in the ocean areas adjacent to South Africa. Deep-Sea Res. 28, 1289–1302.

Lutjeharms, J.R.E., 1996 The exchange of water between the South Indian and South Atlantic Oceans. In: Wefer, G. et al. (Eds.), The South Atlantic: Present and Past Circulation. Springer, Berlin, pp. 125–162.

Lutjeharms, J.R.E., Meeuwis, J.M., 1986. The extent and variability of South-East Atlantic upwellings. S. Afr. J. Mar. Sci. 5, 51–62.

Lutjeharms, J.R.E., Valentine, H.R., 1984. Southern Ocean thermal fronts south Africa. Deep-Sea Res. 31 (12), 1461–1475.

Lutjeharms, J.R.E., Fromme, G.A.W., Valentine, H.R., 1981. Oceanic frontal systems between Africa and Antarctica. Eos Trans. Am. Geophys. Union 62, 942.

Lutjeharms, J.R.E., Ruijter, W.P.M., Peterson, R.G., 1992. Interbasins exchange and the Agulhas retroflection: the development of some oceanographic concepts. Deep-Sea Res. 39 (10), 1791–1807.

Martin, A.K., Flemming, B.W., 1988. Physiography, structure and geological evolution of the Natal Continental Shelf. In Schumann, E.H. (Ed.), Coastal Ocean Studies off Natal, South Africa. Springer, New York, NY, pp. 11–14.

Martin, A.K., Goodlad, S.W., Salmon, D.A., 1982. Sedimentary basin in-fill in the northernmost Natal Valley, hiatus development and Agulhas Current Paleoceanography. J. Geol. Soc. London 139, 183–201.

Martinson, D.G., Pisias, N.G., Hays, J.D., Imbrie, J., Moore, T.C., Shackleton, N.J., 1987. Age dating and the Orbital Theory of the Ice Ages: Development of a high-resolution 0 to 300,000-year chronostratigraphy. Quat. Res. 27, 1–29.

Matsuoka, H., Okada, H., 1990. Time-progressive morphometrical changes of the genus *Gephyrocapsa* in the Quaternary sequence of the tropical Indian Ocean, Site 709. Proc. ODP Sci. Results 115, 255–270.

McIntyre, A., Bé, A.W.H., 1967. Modern Coccolithophoridae of the Atlantic Ocean, placoliths and cyrtoliths. Deep-Sea Res. 14, 561–597.

McIntyre, A., Bé, A.W.H., Roche, M.B., 1970. Modern Pacific Coccolithophorida: a paleontological thermometer. N.Y. Acad. Sci. Trans. Ser. II 32, 720–731.

Mitchel-Innes, B.A., Winter, A., 1987. Coccolithophores: a major phytoplankton component in mature upwelled waters off the Cape Peninsula, South Africa in March, 1983. Mar. Biol. 95, 25–30.

Molfino, B., McIntyre, A., 1990a. Precessional forcing of nutricline dynamics in the equatorial Atlantic. Science 249, 766–769.

Molfino, B., McIntyre, A., 1990b. Nutricline variation in the equatorial Atlantic coinciding with the Younger Dryas. Paleoceanography 5, 997–1008.

Morley, J.J., Hays, J.D., 1979. Comparison of Glacial and Interglacial oceanographic conditions in the South Atlantic from variations in calcium carbonate and radiolarian distributions. Quat. Res. 12, 396–408.

Mostajo, E., 1985. Nanoplancton calcáreo del océano Atlántico Sur. Rev. Esp. Micropaleontol. 77 (2), 261–280.

Niebler, S., 1995. Rekonstruktionen von Paläo-Umwelparametern anhand von stabilen Isotopen und Faunen-Vergesellschaftungen planktischer Foraminiferen im Südatlantik. Ber. Polarforschung 167, 1–198.

Nishida, S., 1986. Nannoplankton flora in the Southern Oceans with special references to siliceous varieties. Mem. Nat. Inst. Polar Res. Spec. Iss. 40, 56–58.

Okada, H., 1980. Calcareous nannofossils from Deep Sea Drilling Project Sites 442 through 446. Philippines Sea. Init. Rep. DSDP 58, 549–565.

Okada, H., Honjo, S., 1973. The distribution of oceanic coccolithophorids in the Pacific. Deep-Sea Res. 20, 355–374.

Okada, H., Honjo, S., 1975. Distribution of coccolithophores in marginal seas along the western Pacific Ocean and in the Red Sea. Mar. Biol. 31 (3), 271–286.

Okada, H., McIntyre, A., 1977. Modern coccolithophores of the Pacific and North Atlantic Oceans. Micropaleontology 23, 1–55.

Okada, H., McIntyre, A., 1979. Seasonal distribution of modern

Coccolithophores in the Western North Atlantic ocean. Mar. Biol. 54, 319–328.

Prell, W.L., Hutson, W.H., Williams, D.F., 1979. The Subtropical Convergence and Late Quaternary circulation in the Southern Ocean. Mar. Micropaleontol. 4, 225–234.

Prell, W.L., Hutson, W.H., Williams, D.F., 1980. Surface circulation of the Indian Ocean during the Last Glacial Maximum, approximately 18,000 yr B.P. Quat. Res. 14, 309–336.

Pujos, A., 1992. Calcareous nannofossils of Plio-Pleistocene sediments from the northwestern margin of tropical Africa. In: Summerhayes, C.P., Prell, W.L., Emeis, K.C. (Eds.), Upwelling Systems: Evolution Since the Early Miocene. Geol. Soc. London Spec. Publ. 64, 33–359.

Pujos-Lamy, A., 1977. *Emiliania* et *Gephyrocapsa* (Nannoplancton calcaire): Biometrie et interet biostratigraphique dans le Pleistocene superieur marin des Açores. Rev. Esp. Micropaleontol. 9, 69–84.

Raffi, I., Backman, J., Rio, D., Shackleton, N.J., 1993. Plio-Pleistocene nannofossil biostratigraphy and calibration to Oxygen Isotope stratigraphies from Deep Sea Drilling Project Site 607 and Ocean Drilling Program Site 677. Paleoceanography 8, 387–408.

Roth, P.H., Berger, W.H., 1975. Distribution and dissolution of coccoliths in the south central Pacific. Cushman Found. Foraminiferal Res. Spec. Publ. 13, 87–113.

Santleben, C., 1980. Die Evolution der Coccolithophoriden-Gattung Gephyrocapsa nach Befunden im Atlantik. Paläont. Z. 54, 91–127.

Sato, T., Takayama, T., 1992. A stratigraphical significant new species of the calcareous nannofossil *Reticulofenestra asanoi*. In: Ishizaki, K., Saito, T. (Eds.), Centenary of Japanese Micropaleontology. Terra Sci. Publ., Tokyo, pp. 457–460.

Schumann, E.H., 1987. The coastal ocean off the east coast of South Africa. Trans. R. Soc. S. Afr. 46 (b), 215–229.

Shackleton, N.J., Berger, A., Peltier, W.R., 1990. An alternative astronomical calibration of the lower Pleistocene timescale based on ODP Site 677. Trans. R. Soc. Edinburgh Earth Sci. 81, 251–261.

Shannon, L.V., Nelson, G., 1996. The Benguela: large scale features and processes and system variability. In: Wefer, G. et al. (Eds.), The South Atlantic: Present and Past Circulation. Springer, Berlin, pp. 163–210.

Shannon, L.V., Agenbag, J.J., Walker, N.D., Lutjeharms, J.R.E., 1990. A major perturbation in the Agulhas retroflection area in 1986. Deep-Sea Res. 37 (3), 493–512.

Strama, L., 1991. Geostrophic transport of the South Equatorial Current in the Atlantic. J. Mar. Res. 49, 281–294.

Strama, L., Peterson, R.G., 1990. The South Atlantic Current. J. Phys. Oceanogr. 20 (6), 846–859.

Sverdrup, H.U., Johnson, M.W., Fleming, R.H., 1942. The Oceans: their Physics, Chemistry and General Biology. Prentice-Hall, Englewood Cliffs, NJ, 1087 pp.

Thierstein, H.R., Geitzenauer, K.R., Molfino, B., Shackleton, N.J., 1977. Global synchroneity of late Quaternary coccolith datum levels: Validation by oxygen isotopes. Geology 5, 400–404.

Villanueva, J., 1996. Estudi de les variacions climatiques y oceanografiques a l'Atlantique Nord durant els ultims 3,000,000 anys mitjançant l'analisi de marcadors moleculars. Ph.D. Thesis, Univ. Ramon Llull, Barcelona 186 pp. (unpubl.).

Warren, B.A., 1981. The shallow oxygen minimum of South Indian Ocean. Deep-Sea Res. 28A (8), 859–864.

Weaver, P.P.E., 1983. An integrated stratigraphy of the Upper Quaternary of the King's Trough flank area EN Atlantic. Oceanol. Acta 6 (4), 451–456.

Waever, P.P.E., Thomson, J., 1993. Calculating erosion by deep-sea turbidity currents during initiation and flow. Nature 364, 136–138.

Wefer, G., Berger, W.H., Bickrt, T., Donner, B., Fischer, G., Kemle-von Mücke, S., Meinecke, G., Müller, P.J., Mulitza, S., Niebler, H.-S., Pätzold, J., Schmidt, H., Schneider, R.R., Segl, M., 1996. Late Quaternary surface circulation of the South Atlantic: The stable isotope record and implications for heath transport and productivity. In: Wefer, G. et al. (Eds.), The South Atlantic: Present and Past Circulation. Springer, Berlin, pp. 461–502.

Wei, W., 1993. Calibration of Upper Pliocene–Lower Pleistocene nannofossil events with Oxygen Isotope stratigraphy. Paleoceanography 8, 85–99.

Wells, P., Okada, H., 1996. Holocene and Pleistocene glacial paleoceanography off southeastern Australia, based on foraminifers and nannofossils in Vema cored hole V18-222. Aust. J. Earth Sci. 43, 509–523.

Wells, P., Okada, H., 1997. Response of nannoplankton to major changes in sea-surface temperature and movements of hydrological fronts over Site DSDP 594 (south Chatham Rise, southeastern New Zealand), during the last 130 kyr. Mar. Micropaleontol. 32, 341–363.

Winter, A., 1982. Paleoenvironmental interpretation of Quaternary coccoliths assemblages from the Gulf of Aqaba (Elat), Red Sea. Rev. Esp. Micropaleontol. 14, 197–223.

Winter, A., Martin, K., 1990. Late Quaternary history of the Agulhas Current. Paleoceanography 5, 479–486.

Ziveri, P., Thunell, R.C., Rio, D., 1995. Export production of coccolithophores in an upwelling region: Results from San Pedro Basin, Southern California Borderlands. Mar. Micropaleontol. 24, 335–358.